DOI:10.25092/baunfbed. 1339334 *J. BAUN Inst. Sci. Technol., 26(2), 431-440, (2024)*

Optimization of contraction cone length in an open-circuit wind tunnel

Seyhun DURMUŞ[1*]

[1]*Balıkesir Üniversitesi, Edremit Sivil Havacılık Yüksekokulu, Balıkesir*

Geliş Tarihi (Received Date): 08.08.2023
Kabul Tarihi (Accepted Date): 04.04.2024

Abstract

The studies in the literature mostly focus on the curvature of the contraction cone, while research regarding the impact of contraction length on flow characteristics is limited. This study aims to determine the optimal length of the contraction cone, which ensures uniform flow at the outlet section, considering the wall shear factor. Four contraction cones of varying lengths were designed based on the hydraulic radius of the inlet. Numerical analysis was conducted to obtain static pressure and velocity distributions for the designed geometries. It was observed that wind tunnels designed with contraction cone lengths 2, 3, and 3.5 times the inlet hydraulic radius exhibited similar flow patterns. However, a longer contraction curve minimizes flow disturbances and turbulence, thereby enhancing flow uniformity and steadiness, while thicker boundary layers result from increased wall shears due to boundary layer growth. Consequently, it was concluded that a wind tunnel configured with a contraction cone length of 2 times the inlet hydraulic radius (square contraction cone) is the optimal choice, considering the combined effects of wall shear and flow uniformity.

Keywords: *Contraction cone length, wind tunnel, nozzle design, flow uniformity, CFD.*

Açık devre rüzgar tünelinde daralma konisi uzunluğunun optimizasyonu

Öz

Bu çalışmada Literatürdeki çalışmalar çoğunlukla daralma konisinin eğriliğine odaklanırken, daralma uzunluğunun akış özellikleri üzerindeki etkisine ilişkin çalışmalar azdır. Çalışma, duvar kesme gerilme faktörünü birlikte dikkate alarak daralma konisinin çıkış bölümünde düzgün akış sağlayan daralma konisinin optimum uzunluğunu ortaya

[*]Seyhun Durmuş, drmsyhn@gmail.com, https://orcid.org/0000-0002-1409-7355

çıkarmayı amaçlamaktadır. Giriş hidrolik yarıçapının uzunluğuna bağlı olarak, farklı uzunlukta dört daralma konisi tasarlanmıştır. Tasarlanan geometriler için sayısal analiz yapılarak statik basınç ve hız dağılımları elde edilmiştir. Giriş hidrolik yarıçapının 2, 3 ve 3,5 katı daralma konisi uzunluğu ile tasarlanan rüzgar tünelinde de benzer bir akış patterni elde edildiği bulunmuştur. Bununla birlikte, daha uzun bir daralma eğrisi, akış bozukluklarını ve türbülansı en aza indirir ve bu, akış düzgünlüğüne yardımcı olur, oysa sınır tabakası büyümesi nedeniyle duvardaki kesme gerilmesi daha kalın sınır tabakası ile sonuçlanır. Bu nedenle, duvar kesme ve akış homojenliğinin birlikte etkisi göz önüne alındığında giriş hidrolik yarıçapının (kare daralma konisi) 2 katı daralma konisi uzunluğu ile yapılandırılmış rüzgar tünelinin en iyi seçim olduğu sonucuna varılmıştır.

Anahtar kelimeler: *Daralma konisi uzunluğu, rüzgar tüneli, nozul tasarımı, düzün akış, HAD.*

1. Introduction

There are many parameters that affect the flow pattern in an open circuit wind tunnel. Among the main parameters are the contraction curve profile, convergent angle, contraction cone length, contraction ratio, diffuser length, diffuser angle, and diffuser area ratio. The existing body of literature primarily directs its attention towards investigating the curvature of the contraction cone within various flow systems. However, there remains a notable scarcity in research concerning the influence of contraction length on flow characteristics.

There are numerous studies in the literature focusing on the curve profile of the contraction cone in wind tunnels. Common curves used for the contraction cone include the Witoszynski curve [1], the bicubic curve, and the fifth-order polynomial curve [2]. The bicubic (two arc) contraction curves were initially suggested by Morel [3], while the fifth-order polynomial was proposed by Bell and Mehta [4]. Zanoun [5] experimentally tested three profiles (fifth-order polynomial contraction, two-cubic arcs, Witoszynski second-order polynomial contractions) and concluded that the fifth-order polynomial contraction performs the best in terms of flow uniformity. Lastra et al. [6] designed a new logarithmic contraction cone profile aimed at achieving flow homogeneity and separation of the boundary layer. Ahmed and Eljack [7] studied five different contraction geometries using computational fluid dynamics (CFD). Hoghooghi et al. [8] (2016) numerically examined Rouse's [9], Bell's [4], and Sargison's [10] nozzle, considering the wall pressure distribution, outlet velocity profiles, and pressure losses. Repeated studies have consistently shown that the contraction curve formed by fifth-order polynomials is the most effective in achieving flow uniformity [11-13].

Very little work has been done on determining the optimal length of the contraction cone. When examining the literature concerning contraction cone length, it is noted that the length of the contraction cone varies between 0.15 and 1 times the inlet hydraulic radius for low-cost wind tunnels [14]. Additionally, Mikhail [15] stated that the contraction section length ranges between 2 and 2.5 times the inlet hydraulic radius. Contraction cones designed as square (where the contraction cone length is 2 times the inlet hydraulic radius) are quite common in the literature [16-17]. In addition to considering the contraction cone length, the effect of the aspect ratio of the contraction cone on flow parameters has also been studied [18]. It is claimed that, to control flow separation, the area ratio of the diffuser should be less than 2.5, and the diffuser angle should be between 5° and 7° [19]. The contraction curve composed of two cubic 5th order polynomials has

repeatedly been verified as the most effective form in achieving flow uniformity [3-4,13]. Additionally, contraction curves generated by sixth-order polynomials have also been examined in the literature [10,20]. Passman et al. [21] studied two-stage contraction cones, consisting of a three-dimensional section and a piece-wise section, aiming to achieve minimal flow deviation.

Lakshman and Basak [22] studied the Brassard's transformed model using OpenFOAM, focusing on airflow uniformity, wall shear stress, and turbulence intensity. Results indicate the transformed model offers better uniformity and turbulence control compared to the original polynomial design. İsmail et al. [23] optimizes the design of an open circuit wind tunnel suction type using TEA (Task Episode Accumulation) and Computational Fluid Dynamics (CFD) with Ansys 15.0. Variation 6 emerges as the best performer, featuring dimensions of 5.015 m length, 15.0 m/s speed, Reynolds number of 8.1 x 10, and turbulence intensity between 10.25-10.75%.

Abdelhamed et al. [24] studied the redesign of the three-dimensional geometry of an open circuit wind tunnel contraction using CFD and optimization tools. The study achieves the recommended contraction ratio, uniformity at the working section, and minimizes boundary layer thickness. Hasselmann et al. [25] applied CFD and a geometrical approach to optimize a piece-wise conical contraction zone in a high-pressure wind tunnel, focusing on minimizing flow deviation and separation.

In the existing literature, the length of the constriction cone is generally taken as 2 times the hydraulic diameter, but the justification for this is always explained based on 1 time the hydraulic diameter; what kind of effects will occur in contraction cones with a length of 3 or 4 times the hydraulic diameter has not been examined in the literature. Thus, the focal objective of this study is to elucidate the optimal length parameter for the contraction cone through a comprehensive Computational Fluid Dynamics (CFD) analysis.

In this investigation, we have designed four distinct lengths for the contraction cones, corresponding to specific inlet hydraulic radius profiles, utilizing a sophisticated 5th degree polynomial approach. Subsequently, employing the ANSYS Fluent CFD Package, we meticulously scrutinized the flow properties associated with each of these contraction cone configurations. Through this detailed analysis, we aim to provide valuable insights into the intricate interplay between contraction length and flow behavior, thereby contributing to the enhancement of engineering practices and fluid dynamics understanding.

2. Material and method

The contraction cone area ratio, contraction curve profile, contraction cone length, diffuser length, and diffuser area ratio are the main parameters that affect the flow properties in an open circuit wind tunnel. A schematic diagram of an open-circuit wind channel is provided in Fig. 1. The optimum area ratio of the contraction cone (A_1/A_2) falls between 6 and 9 in wind tunnels [26]. The area ratio value of the wind tunnel design used in the current study is 8. The minimum diffuser length (L_D) is a function of the inlet hydraulic radius (Ri) and the diffuser angle (θ). Since the optimum total diffuser angle is 6°, a half angle of 3° is used in the present study. The optimum area ratio (A3/A2) ranges

between 2 and 2.5; thus, the value of A_3/A_2 chosen for the current study is 2. The relationship between diffuser length (L_D), hydraulic radius (Ri), optimum area ratio, and diffuser angle (θ) is given in Eq. 1.

$$L_D = R_i \frac{\sqrt{A_3/A_2 - 1}}{\tan(\theta)} \qquad (1)$$

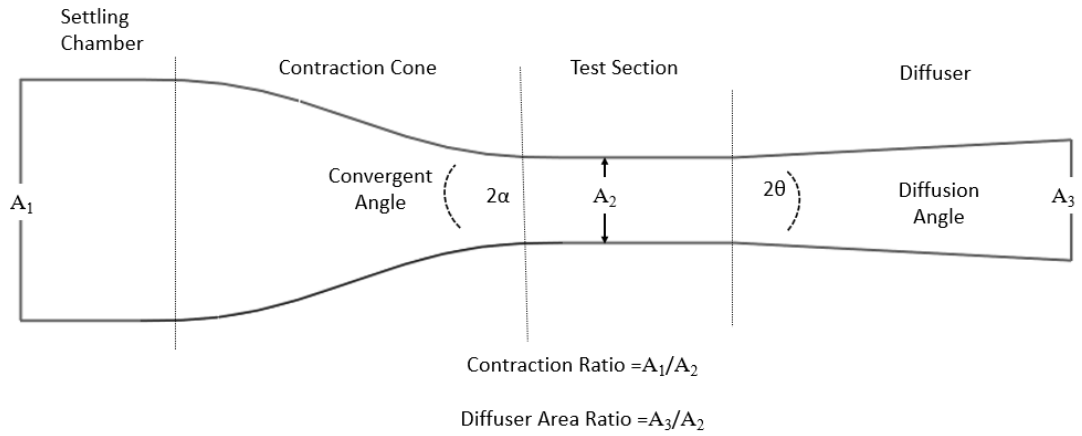

Figure 1. Schematic diagram of an open-circuit wind channel.

The 5th order polynomial proposed by Bell and Mehta [4] for the contraction cone curvature is given in Eq. 2, where h is height of contraction cone, H_i is the inlet height of contraction cone, H_o is the outlet height of contraction cone, and ξ is dimensionless length (X/length).

$$h = (H_i - H_o)\left[-6\xi^5 + 15\xi^4 - 10\xi^3\right] + H_i \qquad (2)$$

The study aimed to determine the optimum contraction cone length (L_{CC}) according to the outlet velocity distribution of the contraction cone through CFD analysis. The design properties of the wind tunnel are provided in the Table 1.

Table 1. Design properties of wind tunnel

Parameter List	**Value**
Inlet hydraulic radius (R_i)	70.71 cm
Contraction ratio (A_1/A_2)	8
Contraction cone lengths (L_{CC})	R_i, $2R_i$, $3R_i$, $4R_i$
Contraction cone angle (2α)	2x10.5 °
Test section height X length	0.5 m X 1 m
Total diffuser angle (2θ)	6°
Area ratio of diffuser (A_3/A_2)	2
Diffuser length	197.59 cm

Fig. 2 displays the curves of the lower wall of the contraction cones obtained using the 5th order polynomial. Since the test length is set at 50 cm, the corresponding height of the

contraction cone is calculated as 45.71 cm. The length of the contraction cone is determined based on the inlet hydraulic radius (R_i) and this value is 70.71 cm. During the design process of the computer-aided drawing of the wind tunnel section, the length of the settling chamber was set to R_i (70.71 cm), and the length of the test section was fixed at 50 cm.

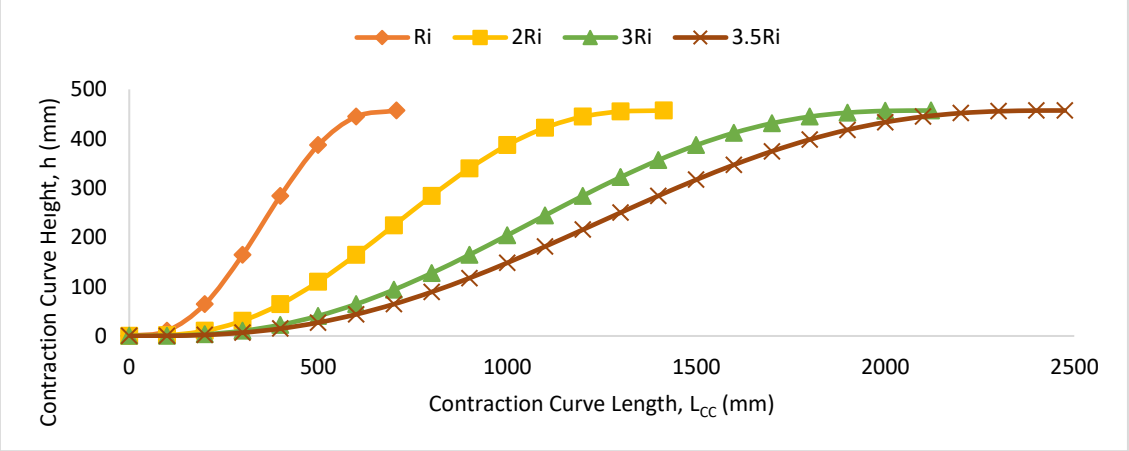

Figure 2. Contraction cone profiles with different lengths obtained with the 5th order polynomial proposed by Bell and Mehta [4].

ANSYS Fluent CFD package was used for numerical simulation, while the CFD-Post package was employed for monitoring of analysis results. The continuity equation and conservation momentum are the primary governing equations and the governing equation groups were discretized with second order scheme and SIMPLEC algorithm were used. The standard k−ε turbulence model was selected to model turbulence in wind tunnels as it is widely used in such studies in the literature [7,12]. John et al. [27] were employed turbulence models such as the k-ε, k-ω, RSM, SST k-ω, and LES. Simulation outcomes reveal that the k-ε model yields the lowest turbulence intensity. Therefore, in this study, this model was deemed more appropriate to work. The convergence criterion was set to 1×10^{-4}. The mass flow inlet boundary condition was applied for settling chamber inlet and mass flow outlet boundary condition was selected for diffuser outlet. The no slip condition was selected as boundary for walls. A grid independence test was performed considering the static pressure values. Mesh sensitivity test is given in Table 2. All quad mesh options with the fine (node numbers=1200X1200), medium mesh (900X900) and coarse (node numbers=600X600) mesh options were applied to a chosen profile (L_{CC}=3R_i) and analyses were performed with the fine mesh option.

Table 2. Mesh sensitivity test.

	Coarse Mesh	Medium Mesh	Fine Mesh
Node Number	600X600	900X900	1200X1200
Static pressure at midline of outlet region of test section	-516.2 Pa	-514,1 Pa	-513.3 Pa
Change in result.	0.57%	0.15%	-

Recognizing that the mesh in the near-wall region strongly affects the wall shear, a higher density mesh near the tunnel walls was implemented. The consideration for the near-wall mesh (y+) ensured that the first cell adjacent to the contraction cone wall remained under 1.

3. Results

In the research findings of numerical analysis, static pressure and velocity distribution contours were obtained for four types of wind tunnels with different lengths of contraction cones. Static pressure distributions for contraction cones of different lengths are shown in Fig. 3. In the test section, the static pressure values decreased significantly and recovered in the diffuser section, but due to losses it reaches a value lower than initial value. An obvious difference was observed in static pressure changes in the vertical direction of outlet of contraction cone. In the first design ($L_{CC}=R_i$) very low static pressure values are observed locally on the walls of the contraction cone for the and sudden pressure losses are partially observed in the second design ($L_{CC}=2R_i$). A more uniform pressure distribution occurs in the 3rd ($L_{CC}=3R_i$) and 4th ($L_{CC}=3.5R_i$) design case. Average static pressure distribution values along the symmetry (mid-section) line are similar for the 3rd design ($L_{CC}=3R_i$) and the 4th ($L_{CC}=3.5R_i$).

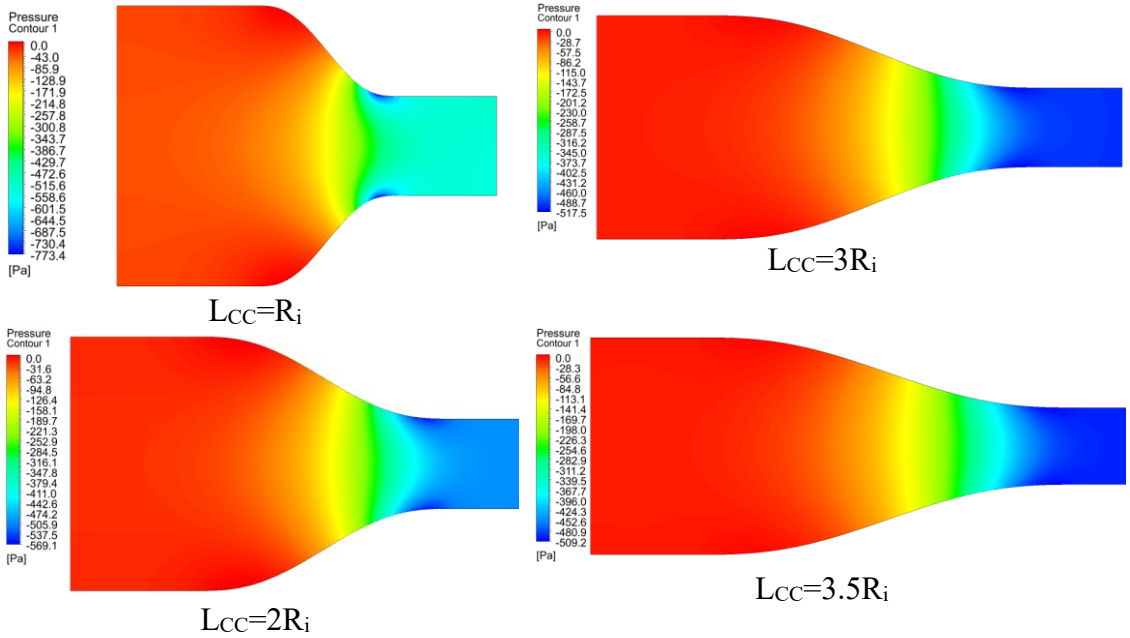

Figure 3. Static pressure distribution contours in contraction cones of different lengths

Velocity contours of contraction cones of different lengths are depicted in Fig. 4. Regarding velocity values, the highest velocity value is observed in the test section, while the velocity decreases slightly in the diffuser. Although the velocity magnitude values are not locally homogeneous in the first design, depending on the sudden pressure losses, it is possible to talk about a more uniform velocity distribution for the third design ($L_{CC}=3R_i$) and fourth design ($L_{CC}=3.5R_i$). The velocity magnitudes values are more regular at the outlet of the test section. However, the speed values are relatively more irregular at the exit of the contraction cone, specifically at the entrance of the test section.

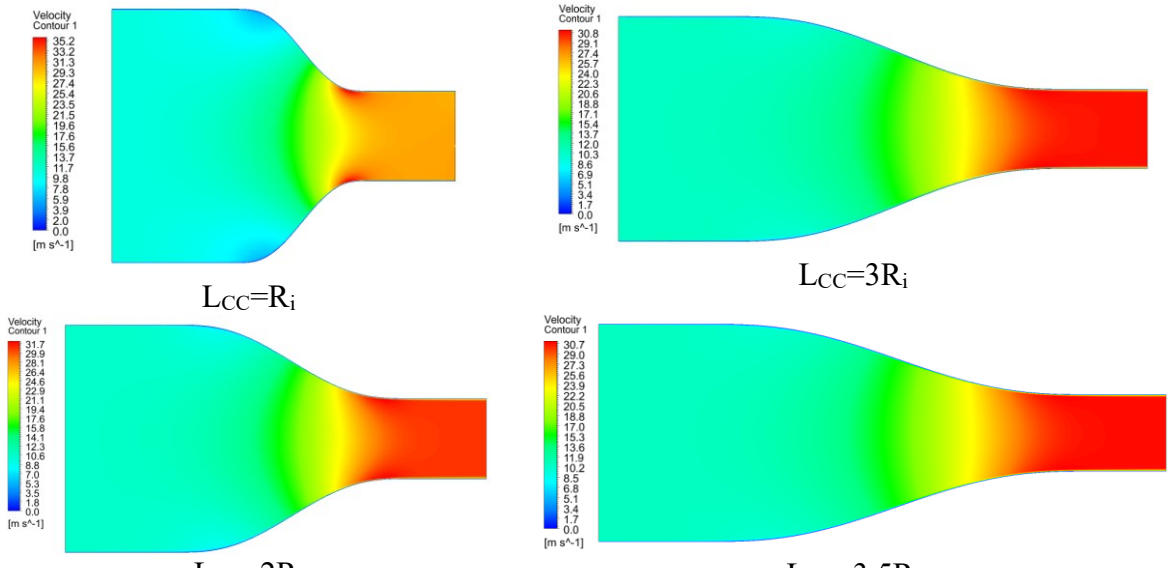

Figure 4**.** Velocity distribution contours in contraction cones of different lengths

Whether the optimum contraction cone length is advantageous can be questioned based on the uniformity of the velocity distributions at the outlet section of the contraction cone. The distribution of the velocity components taken from the vertical axis (Y axis) at the outlet section of the contraction cone of all cases is shown in Fig. 5. To discern the differences between the velocity values, the image is provided with zooming. It can be observed that the contraction cone with $L_{CC}=3R_i$ and $L_{CC}=3.5R_i$ provide more uniform flow pattern, considering the velocity inlet profile of the test section. The results presented in Fig. 5 align well with the findings from a study conducted by Arifuzzaman and Mashud, specifically involving a square contraction cone, as referenced by [14].

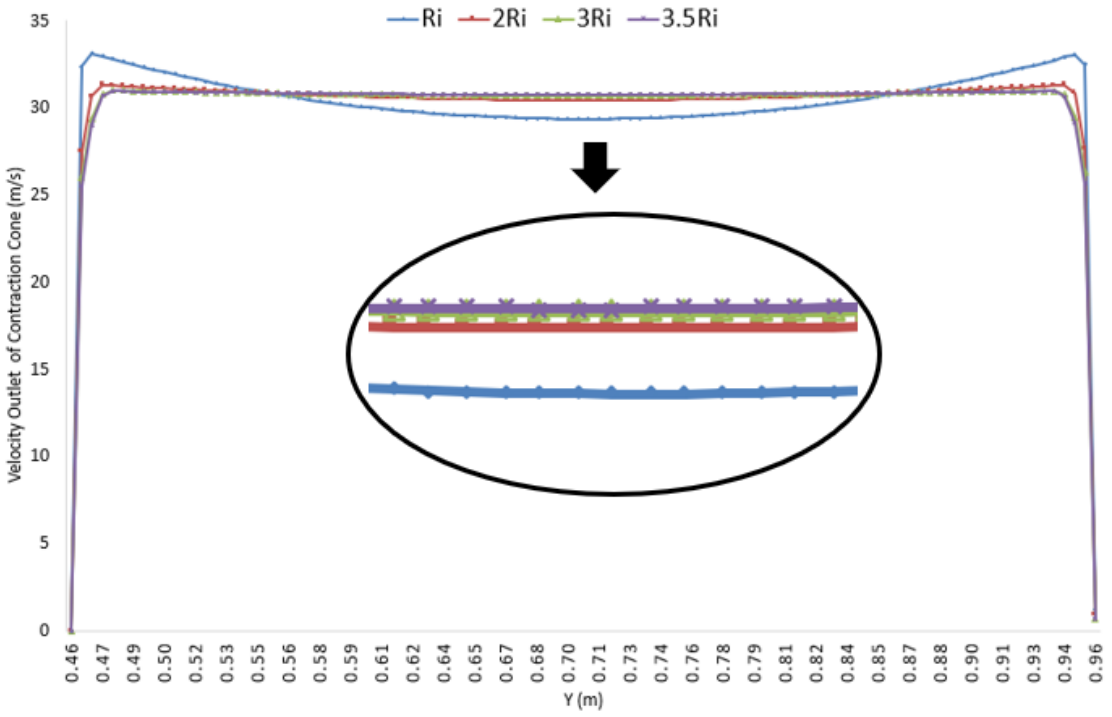

Figure 5. Outlet velocity profile of contraction cones with different lengths

Furthermore, the presence of a longer contraction curve mitigates the impact of wall shears caused by boundary layer growth. In fluid dynamics, as fluid moves along a surface, such as the walls of a conduit, a thin layer of fluid called the boundary layer forms [11]. This boundary layer can grow thicker as the flow progresses, leading to increased wall shears. However, with a longer contraction curve, the boundary layer growth is more gradual, resulting in a thinner boundary layer and reduced wall shears. According to the computational fluid dynamics (CFD) analysis results, it appears that a contraction length-to-diameter ratio of 3.5 times the radius of the inlet (L_{CC}=3.5Ri) initially seems to offer the most favorable conditions. However, it is noted that this configuration suffers from a disadvantageous increase in wall shear due to the thicker boundary layer associated with its longer length. Therefore, despite its seemingly optimal flow characteristics, the L_{CC}=3.5Ri design is deemed less desirable due to the heightened wall shear. Consequently, the configuration with an L_{CC} of 2 times the radius of the inlet (L_{CC}=2Ri), represented by a square contraction cone, emerges as the superior choice when considering both the effects of wall shear and flow uniformity in tandem. In summary, a longer contraction curve proves advantageous in minimizing flow disturbances and turbulence, as well as reducing the impact of wall shears caused by boundary layer growth. Despite initially appearing optimal, the design with the longest contraction curve is ultimately deemed less favorable due to increased wall shear, leading to the selection of a shorter contraction curve configuration for optimal flow uniformity and steadiness.

4. Conclusion

In the study, numerical analyzes were performed for the design of the contraction cone with 4 different lengths in order to determine the optimum length of the contraction cone that provides smooth flow in test section of wind tunnels. The results present pressure and velocity distribution contours for the four design cases. The optimal geometry value is determined based on the criterion of achieving uniform velocity distributions at the outlet of the contraction cone. It was found that flow forms were not uniform in the contraction cones designed with L_{CC}=R_i. However, uniform flow forms were obtained in contraction cones designed with LCC=2Ri, L_{CC}=3 R_i and L_{CC}=3.5 R_i. Nonetheless, a longer contraction curve minimizes flow disturbances and turbulence, thereby enhancing flow uniformity and steadiness. However, the increase in wall shears due to boundary layer growth results in a thicker boundary layer. Therefore, the L_{CC}=2R_i configuration (square contraction cone) is considered the best choice, considering the combined effects of wall shear and flow uniformity.

Nomenclature

A_1	area of contraction cone inlet of wind tunnel
A_2	area of contraction cone outlet of wind tunnel
A_3	area of diffuser outlet of wind tunnel
D	inlet diameter of venturi tube
d	throat diameter of venturi tube
H_i	inlet height of contraction cone
H_o	inlet height of contraction cone
L_{CC}	contraction cone length
L_D	minimum diffuser length
R_i	inlet hydraulic radius

y+ dimensionless near wall distance
α convergent angle
θ Diffuser angle
ξ dimensionless length value of contraction cone

References

[1] Witoszynski, C., Votraege aus dem gebiet der hydro- und aerodynamik, aus Stroemungstechnisches Messwesen bei S.G. Popow, **VEB Verlag Techni**k Berlin, (1960).

[2] Li, H., Chen, C., Liu, B., & Zhang, L., Flow quality analysis of contraction section and test section of low-speed wind tunnel based on CFD numerical simulation. **Journal of Physics: Conference Series,** vol. 1176, no. 5, p. 052064. IOP Publishing, (2019).

[3] Morel, T. Design of two-dimensional wind tunnel contractions. **ASME Journal of Fluids Engineering**, vol. 99, pp. 371-378, (1977).

[4] Bell, J. H., and Mehta, R. D. Contraction Design for Small Low Speed Wind Tunnels. **NASA Contractor Rep. No. NASA-CR-177488**, (1988).

[5] Zanoun, E. S. Flow characteristics in low-speed wind tunnel contractions: Simulation and testing. **Alexandria engineering journal,** vol. 57, no. 4, , pp. 2265-2277, (2018).

[6] Lastra, M. R. et al. Novel design and experimental validation of a contraction nozzle for aerodynamic measurements in a subsonic wind tunnel. **Journal of Wind Engineering and Industrial Aerodynamics**, vol. 118, pp. 35-43, (2013).

[7] Ahmed, D. E., & Eljack, E. M. Optimization of model wind-tunnel contraction using CFD. International Conference on Heat Transfer, **Fluid Mechanics and Thermodynamics,** (2014).

[8] Hoghooghi, H., Ahmadabadi, M. N., & Manshadi, M. D. Optimization of a subsonic wind tunnel nozzle with low contraction ratio via ball-spine inverse design method. **Journal of mechanical science and technology**, vol. 30, no. 5, pp. 2059-2067, (2016).

[9] Rouse, H. Cavitation-free inlets and contractions (Electrical analogy facilitates design problem). **Mech. Engng.,** vol. 71, pp. 213-416, (1949).

[10] Sargison, J. E., Walker, G. J., & Rossi, R. Design and calibration of a wind tunnel with a two dimensional contraction., **15th Australasian Fluid Mechanics Conference**, The University of Sydney, Sydney, Australia, (2004).

[11] Barlow, J. B., Rae, W. H., & Pope, A. Low-speed wind tunnel testing. **John Wiley & Sons**, (1999).

[12] Doolan, C. J. Numerical evaluation of contemporary low-speed wind tunnel contraction designs., **J. Fluids Eng.** (2007).

[13] Ramaeshan, S., Ramaswamy, M.A. A rational method to choose optimum design for two dimensional contractions. **ASME Journal of Fluids Engineering**, vol. 124, pp. 544-546, (2002).

[14] Arifuzzaman, M., & Mashud, M. Design construction and performance test of a low cost subsonic wind tunnel. **IOSR Journal of Engineering**, vol. 2, no. 10, pp. 83-92, (2012).

[15] Mikhail, M. N. Optimum design of wind tunnel contractions**. AIAA journal**, vol. 17, no. 5, pp. 471-477, (1979).

[16] Fang, F. M., Chen, J. C., & Hong, Y. T. Experimental and analytical evaluation of flow in a square-to-square wind tunnel contraction. **Journal of Wind Engineering and Industrial Aerodynamics,** vol. 89, no. 3-4,pp. 247-262, (2001).

[17] Liu, J. S. Numerical Simulation and Optimization of Small low-speed Wind Tunnel Contraction flow. **Applied Mechanics and Materials**, vol. 733, pp. 595-598. Trans Tech Publications Ltd., (2015).

[18] Callan, J., & Marusic, I. Effects of changing aspect ratio through a wind-tunnel contraction. **AIAA journal**, vol. 39, no. 9, pp. 1800-1803, (2001).

[19] Mikel, Russell, ed. Wind Tunnels: Models, Aerodynamics and Applications. **Clanrye International,** (2015).

[20] Javed, K., & Ali, M., Design & Construction of subsonic wind Tunnel focusing on two-dimensional contraction cone profile using sixth order polynomial., **Scientific Cooperations International Workshops on Engineering Branches**,(2014)

[21] Passmann, M., Reinker, F., Hasselmann, K., aus der Wiesche, S., & Joos, F., Development and Design of a Two-Stage Contraction Zone and Test Section of an Organic Rankine Cycle Wind Tunnel. In Turbo Expo: Power for Land, Sea, and Air (Vol. 49743, p. V003T25A006). **American Society of Mechanical Engineers**, (2016).

[22] Lakshman, R., and Ranjan Basak. Analysis of transformed fifth order polynomial curve for the contraction of wind tunnel by using OpenFOAM. **IOP conference series: materials science and engineering.** Vol. 377. No. 1. (2018).

[23] Ismail, J., et al. Optimization Design of Open Circuit Wind Tunnel Suction Type. **Int. J. Mech. Mechatronics Eng** 17.06 121. (2017).

[24] Abdelhamed, A. S., Y. El-S. Yassen, and M. M. ElSakka. Design optimization of three dimensional geometry of wind tunnel contraction. **Ain Shams Engineering Journal**. 6,1. 281-288. (2015).

[25] Hasselmann, Karsten, et al. Numerical optimization of a piece-wise conical contraction zone of a high-pressure wind tunnel. **American Society of Mechanical Engineers**, Vol. 57212. 2015.

[26] Bradshaw, P., Pankhurst, R. C., The design of low-speed wind tunnels. **Progress in Aerospace Sciences**, 5, 1-69, (1964).

[27] John, Johanis, İsmail.İ., Pane E. Computational fluid dynamics simulation of the turbulence models in the tested section on wind tunnel. **Ain Shams Engineering Journal** 11.4 1201-1209. (2020).